Journal of Hazardous Materials 239–240 (2012) 241–248

Contents lists available at SciVerse ScienceDirect

Journal of Hazardous Materials

journal homepage: www.elsevier.com/locate/jhazmat

Proteome pattern in oysters as a diagnostic tool for metal pollution

Fengjie Liu, Wen-Xiong Wang*

Division of Life Science, The Hong Kong University of Science and Technology (HKUST), Clear Water Bay, Kowloon, Hong Kong

HIGHLIGHTS

- Principal components analysis revealed that the oysters had distinct contamination profiles.
- Proteomic analysis identified a proteome pattern composed of 13 commonly altered proteins in the contaminated oysters.
- The proteome pattern could classify the oysters with different comtanination levels.
- The integrated proteome change were linearly related to the integrated contamination of the metal mixtures.
- Proteome pattern is a promising diagnostic tool for metal pollution assessment.

ARTICLE INFO

Article history:
Received 10 May 2012
Received in revised form 27 August 2012
Accepted 28 August 2012
Available online 4 September 2012

Keywords:
Multiple-metal pollution
Oyster
Protein expression signature
Proteomics
Pollution assessment

ABSTRACT

The present study investigated whether proteome pattern of an oyster *Crassostrea hongkongensis* could be used as a diagnostic tool for contamination and toxicity of metals/metalloids in a real multiple metal-contaminated estuary. We collected oysters along a pollution gradient from highly contaminated to relatively clean sites. The oysters showed distinct contamination gradients of Cu, Zn and Cd. Proteomic analysis of the oyster gills as one of major metal targets identified a proteome pattern composed of 13 commonly altered proteins in the contaminated oysters. The discovered proteome pattern completely segregated the contaminated from the clean individuals, and the pattern achieved clear classification of the oysters with different contamination levels. Importantly, the integrated changes of gill proteome were linearly related to the integrated contamination of the metal mixtures present in oyster tissues. It is suggested that proteome pattern is a promising diagnostic tool for metal pollution assessment in environmental monitoring programs.

1. Introduction

The ecological effects of thousands of anthropogenic chemicals on aquatic ecosystems have become a major concern, and many metal contaminants are on the high priority lists of hazardous substances (e.g., As, Cd, Cr, Cu, Hg, Pb, Zn). Excessive loading of anthropogenic metals into aquatic environment has caused inestimable adverse impacts on ecosystems and human beings. Successful ecological monitoring relies on our ability to timely identify the major pollutants and to accurately predict the consequences; both of which rely on a comprehensive understanding of environmental behaviors and mode of action of these pollutants [1]. For decades, bivalves have been widely employed to monitor metal contamination in coastal waters worldwide, as their tissue metal concentrations can integratedly reflect the bioavailability of metals in the environment [1–3].

To spot early molecular events involving in toxicant responses, biomarkers (signs associated with toxicant exposure at the lower levels of biological organization) are generally measured [4,5]. Unfortunately, few of the established biomarkers have adequate sensitivity, specificity, and predictive value for metal contamination. Even the use of traditional biomarkers requires a comprehensive knowledge of the interactions between contaminants and organisms [6–9]. For example, metallothioneins (MTs), low-molecular-weight metal-binding proteins, are the most widely used biomarkers in environmental monitoring programmes. However, the best MTs as metal biomarkers are still a subject of discussion, because both field and laboratory studies showed the difficulty of MTs in discriminating metal-polluted and clean animals [10,11]. Furthermore, metal pollutants rarely occur alone, and most of contaminated waters are enriched with mixtures of metals [1,12]. Predicting the toxic effects of metal mixtures based on a single biomarker is a great challenge due to their complex effects caused by concentration additivity or synergism, and at present there are no effective molecular diagnostic tools for mixture exposure [9]. Thus, application of new concepts

* Corresponding author. Tel.: +852 2358 7346; fax: +852 2358 1559.
E-mail address: wwang@ust.hk (W.-X. Wang).

0304-3894/$ – see front matter © 2012 Elsevier B.V. All rights reserved.
http://dx.doi.org/10.1016/j.jhazmat.2012.08.069

and technologies for detection and prediction of metal mixture exposure is highly demanded [9,12].

Nowadays, there is an increasing awareness that the analysis of an organism's proteome allows the detection of a total set of proteins' change in response to environmental contaminants [7,8,13,14]. Importantly, pattern changes of biomonitor proteome might reflect the levels of contamination and toxic effects on aquatic animals, thus proteome pattern might represent a new diagnostic paradigm in environmental pollution assessment. Proteome patterns have been determined in several organisms exposed to metals and other abiotic stressors [15–20], and the identified patterns allowed distinguishing animals from clean and polluted sites [17,21]. The application of this concept in ecotoxicology has grown steadily, but there is a general lack of field validation to demonstrate the relationships between contamination/toxicity and proteome response [8,16,17,22,23].

The present study aimed to demonstrate the usefulness of proteome pattern in aquatic invertebrates as a diagnostic tool for contamination and toxicity of metals/metalloids in a real multiple metal-polluted estuary (i.e., the Jiulongjiang estuary), which was contaminated by several metals/metalloids [24,25]. Proteome pattern was generated from the gills of these native contaminated oysters *Crassostrea hongkongensis*, which were collected along a pollution gradient in the estuary, as the gill is a major metal storage and target organ [24]. The discovered pattern was then used to blindly classify the oysters with different contamination levels from highly contaminated to relatively clean sites. We hypothesized that the proteome of the more contaminated oyster might have changed more than that of the less contaminated one, in comparison to the proteome of the clean one, and the proteome pattern of the more contaminated one showed less similarity to that of the clean one. Proteome pattern may be a good indicator of integrated contamination (possibly toxic effect) of metal mixtures to the species. Besides, the significantly altered protein spots were putatively identified by homology searches following MS/MS analysis to gain insights into the underlying mechanisms of toxic effects of multiple-metal exposure, although genetic information of the oyster is not available yet.

2. Materials and methods

2.1. Oyster sampling

During the low tides, the native contaminated oysters *C. hongkongensis* were collected from the Gongqian (GQ, 24°24′15″N, 117°57′5″E) and Baijiao (BJ, 24°28′9″N, 117°55′59″E) sites along the contaminated Jiulongjiang estuary, and the control oysters *C. hongkongensis* were collected from the Zhangpu (ZP, 24°2′15″N, 117°43′8″E) site from the nearby relatively clean Jiuzhen estuary, Fujian of China, on December 18th–22th, 2010. Previous studies suggested that the Jiulongjiang estuary was contaminated with metals [26,27], but it was recently documented that the concentrations of sediment metals were elevated, especially for Cu and Zn [24]. In addition, the Jiulongjiang estuary had much higher labile dissolved concentrations of Cu, Zn and Cd than the reference ZP site, as revealed by the measurements using diffusive gradients in thin film units [25]. These findings were consistent with the increasing industrialization in the rapidly developing area. In addition, there was no noticeable contamination of organic contaminants, including PCBs and PAHs, in the Jiulongjiang estuary [28–31]. The estuary was an important area for oyster culture, and the average surface salinity ranged from 14 to 26 psu as for tidal actions. Twelve individuals of similar size were selected from each site, and the gills were immediately dissected after being rinsed with Milli-Q water for at least three times. There was no osmotic shock during the washing process. Four individual gills from the same site were pooled together, and there were three biological replicates of different pooled samples. Subsequently, the gills were homogenized in a 3-mL 10% trichloroethanoic acid (TCA)/acetone (w/v) buffer placing in an ice-water bath. One mL of the homogenate was used for metal analysis while the remaining was subjected to proteomic analysis.

2.2. Metal analysis

The gill homogenate, remaining tissues of the oysters and similar weight samples of the certified standard reference material 1566b-oyster tissue were freeze-dried and thoroughly digested in concentrated HNO_3. The digests were subsequently diluted to appropriate concentration ranges with a 2% HNO_3 solution. The procedures were carried out in a clean hood, and trace metal clean reagents and techniques were used throughout the digestion procedures. The metals/metalloid (Ag, As, Cd, Cr, Cu, Ni and Zn) in the digests were determined by inductively coupled plasma-mass spectrometry (ICP-MS, Agilent 7700×), and the instrument was calibrated with external standards. To account for instrument drift and change in sensitivity, internal standardization was also performed by addition of Sc, Ge, Y, In, Tb and Bi (Internal Standard Mix Part# 5183-4681, Agilent) to the samples and standards. One of the standards was reanalyzed after every 30 samples, and deviations from the standard value were in general less than 10% for the elements. The levels of the detection limit for the metals/metalloid, calculated from replicate blank analyses, were several orders of magnitude below the concentrations determined in the oyster samples. The recovery percentage from the reference standard oyster tissue was 98–105%, and there was no certificated value for Cr in the reference material. The metal/metalloid concentrations were reported as μg metal/metalloid per g wet weight tissue.

2.3. Proteomic analysis

The gill proteome was visualized by a silver staining method compatible with MS analysis, and the detailed procedures are described in our previous study [32]. The silver staining allows for detection of <1 ng protein per spot, and the method has proven effective in quantification and mass spectrometric sequencing of proteins [21,32,33]. Briefly, the gill proteins were extracted in 10% trichloroethanoic acid/acetone (w/v) buffer, and protein concentration was determined by a 2-D Quant Kit assay (GE Healthcare). Then, the extracted proteins were separated by two-dimensional electrophoresis (2-DE), and the digitized 2-DE images (Bio-Rad GS-670) were analyzed with ImageMasterTM 2D Platinum (Amersham Biosciences). Protein abundance was defined as normalized relative volume of protein spots (% of the total spot volume), and a higher normalized volume of a spot in one gel in comparison to that in the corresponding control gel reflects a higher concentration of the protein.

The interesting proteins were putatively identified by homology searches following MS/MS analysis as described in the previous study [32], since the genetic information of the oyster is not available yet. Briefly, differentially expressed protein spots were digested with trypsin, and peptides were extracted with 50% acetonitrile plus 0.1% trifluoroacetic acid. The MS and tandem MS data were acquired in a positive MS reflector mode with a scan ranging from 800 to 4000 Da, and the 20 most intense precursors were further fragmented in collision-induced decomposition mode. Finally, the data were submitted to the search engine Mascot for homology searches against the NCBInr and the bivalvia EST database. Similarity was not considered to be significant when the protein score C.I.% was less than 95 (for search in the NCBInr) or *E*-value was more than e^{-20} (for search in the bivalvia EST). The identified proteins were

Table 1
Metal/metalloid concentrations in the gill of the oysters *Crassostrea hongkongensis* collected from three estuarine sites.

Sampling site	Gill metal/metalloid concentration (μg/g wet weight)						
	Cu	Zn	Cd	Ag	Ni	Cr	As
ZP	67.2 ± 43.6	272.8 ± 114.4	0.7 ± 0.1	1.5 ± 0.8	1.2 ± 0.4	5.1 ± 4.1	2.5 ± 0.1
GQ	211.2 ± 34.7*	1359.8 ± 173.6*	4.0 ± 0.8*	0.7 ± 0.1*	2.1 ± 0.6*	12.2 ± 3.2*	3.0 ± 0.1*
BJ	1482.6 ± 237.0*	3282.2 ± 93.7*	7.7 ± 4.0*	2.2 ± 0.8	2.5 ± 0.9*	4.1 ± 2.4	1.5 ± 0.3*

Data are mean ± standard deviation ($n = 3$).
* indicates significant difference with that in the ZP ($P < 0.05$, Student t-test).

searched in the Gene Ontology (http://www.geneontology.org/) to infer their possible biological functions.

2.4. Multivariate statistical analyses

Principal components and hierarchical clustering analyses (SPSS 16.0) were used to determine if there were meaningful differences in both the contamination gradients of the metals/metalloid and the expression patterns of proteome [34,35]. The data were normalized by doing a transformation of $(x - \text{mean})$/standard deviation before the multivariate analyses, and thus all the variables had zero mean and unit variance. Differences in the patterns of metals/metalloid among the oysters may reflect variations in the anthropogenic sources or contamination levels. In the present study, the first two principal components had more than four loadings greater than 0.6, and so the PCA analysis was reliable regardless of the sample size [35]. The score plots can give a better indication of the similarity of metals/metalloids contamination gradients in the oysters than a comparison between individual metals/metalloids.

3. Results and discussion

3.1. Contamination pattern of metals/metalloid in the oysters

The gill of bivalves is one of the major targets in storage, toxicity and detoxification of the metals/metalloids [1,24]. The concentrations of six metals (Ag, Cd, Cr, Cu, Ni and Zn) and one metalloid (As) in the gills of the oysters *Crassostrea hongkongenesis* collected from the contaminated and clean sites are summarized in Table 1, and the residual tissues contained similar metal/metalloid concentrations to the gills (data not shown). The concentrations are reported as microgram of metal/metalloid per gram wet weight of oyster tissue, since the maximum acceptable concentrations for metals in molluscan shellfish are established on a wet weight basis [36]. The concentrations of metals in the GQ and BJ oysters were high, particularly in the BJ ones. Concentrations of Cu were as high as 1756 μg/g, and Zn concentrations were as high as 3376 μg/g, whereas Cd concentrations were as high as 10.9 μg/g. The concentrations of Cu, Zn and Cd in the BJ animals were enriched 22, 12 and 11 times relative to the average reference metal levels in the clean ZP oysters, respectively. The BJ and GQ were contaminated to a less extent by Ag, Ni, Cr and As. Interestingly, the contamination profile of the BJ population differed from that of the GQ; the latter contained significantly less Cu, Zn, Cd, Ag but more Cr and As than the BJ one ($P < 0.01$, Student t-test). The concentrations of metals/metalloid measured in the oysters in this study were consistent with a recent study of the oysters in this estuary [24].

To better distinguish the contamination gradients, principal components analysis (PCA) were used to make comparisons of the oysters with respect to seven variables (i.e., six metals and one metalloid). The score plot of the metal content in the oysters is shown in Fig. 1. Together, the first two principal axes retained 85.6% of the variance from the original seven dimensions. In the score plot, three contamination gradients between the populations were evident, and the oysters from the same sampling site clearly clustered together. Specifically, the first principal component separated the contaminated oysters of GQ and BJ from the 'clean' ZP ones, and the second principal component further separated the oysters from the two contaminated sites. The less contaminated GQ oysters had positive loadings along the second principal component, whereas the highly contaminated BJ oysters had negative loadings along the second principal component. Using the information from all the seven contaminants, it was apparent that there were different gradients of metal/metalloid contamination in the oysters.

To evaluate integrated contamination level of the metals/metalloid, a simple equation is proposed:

$$\text{Integrated metal contamination} = \sum_{i=0}^{m} C^i_{\text{contaminated}} - C^i_{\text{clean}}$$

where $C^i_{\text{contaminated}}$ is the concentration of the ith metal/metalloid in a contaminated oyster, and C^i_{clean} is a reference value for the ith metal/metalloid in an uncontaminated one. The reference was determined from the clean ZP oysters collected from a clean site in the present study. The lowest concentrations of the metals/metalloid in the clean oysters were 17 μg/g for Cu, 145 μg/g for Zn, 0.7 μg/g for Cd, 0.6 μg/g for Ag, 0.8 μg/g for Ni, 1.3 μg/g for Cr, 1.3 μg/g for As on a wet weight basis. And, m is the number of all metals/metalloids that an organism were simultaneously exposed to, i.e., $m = 7$ in the present case. We found that the calculated integrated contamination of the oysters was in the following order: the BJ oysters > the GQ oysters > the ZP oysters, which is in good agreement with the pollution gradient of the estuary [24].

3.2. Expression pattern of proteome in the oysters

As oyster gills are the major metal/metalloid target organs [24], gill proteomes of the oysters were visualized by 2-D electrophoresis. Three representative 2-D gels are shown in Fig. 2, and each gel yield about 1200 well-resolved protein spots (observed pI 4–7, observed molecular weight 10–100 kDa). In comparison with the

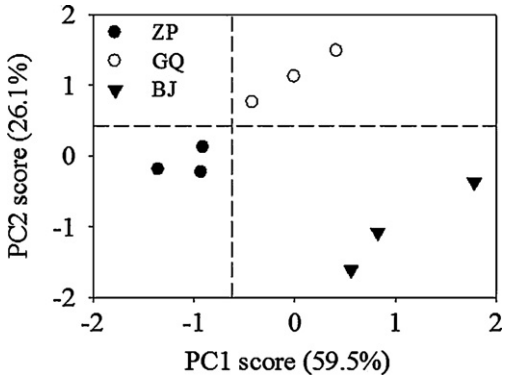

Fig. 1. Principal component score plot of the oyster samples from metal-contaminated (GQ and BJ) and clean (ZP) sites in the new coordinate space defined by the first two principal components (PC). The retained variance of each principal component is shown in parentheses.

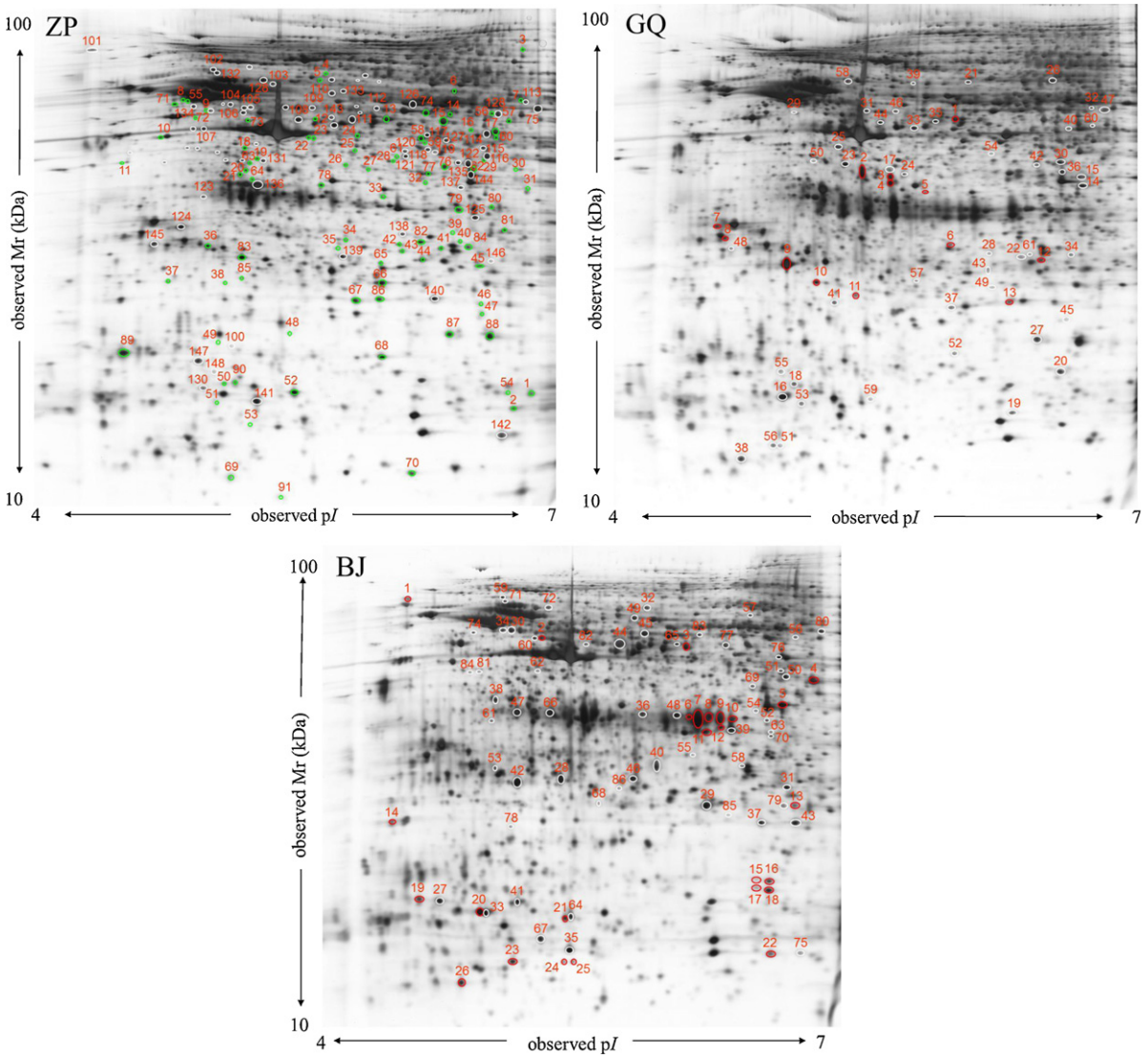

Fig. 2. Representative two-dimensional electrophoresis gels of the gill of the oysters from metal-contaminated (GQ and BJ) and clean (ZP) sites. A protein spot marked with a circle indicates its differential expression in the GQ or BJ oysters in comparison with that in the ZP ($P < 0.05$, Student t-test). The green circles indicate the spots were not detectable in the GQ or BJ oysters, while the red ones indicate the newly appearing spots in the GQ or BJ oysters.

ZP's gels, 63 and 123 protein spots were differentially expressed in abundance in the GQ and BJ ones, respectively ($P < 0.05$, Student t-test), and 13 of the altered protein spots were commonly altered in the contaminated GQ and BJ oysters (Fig. 3A). Expression abundances of the 13 protein spots are shown in Fig. 3B, and none of them was successfully identified at present. Specifically, 11 out of the 13 spots showed lower expression in both the GQ and BJ oysters than those in the ZP ones, whereas one spot of protein ID 130 was significantly over-expressed in the two contaminated populations ($P < 0.05$, Student t-test). It is likely that the 13 proteins were associated with exposure of the metals/metalloid, although at present it is difficult to identify them and to establish their direct causal relationships. Moreover, multiple time periods analyses and potential influences of other environmental variables (e.g., salinity, pH, and temperature) should be taken into account in further field trials in order to develop specific and sensitive biomarkers of metal exposure. Recently, it is reported that unique protein expression profiles of oyster haemolymph exposed to metal contamination in the field were associated with different combinations and concentrations of metals and other environmental variables (predominantly salinity and pH) present during three field trials [23].

Our first question was whether the expression pattern of gill proteome could distinguish the contaminated oysters from the clean ones, and whether it could further classify the contaminated oysters with different contamination levels. Actually, many pathology studies have shown the feasibility of disease diagnosis and prediction based solely on the molecular expression patterns, independent of biological knowledge of the molecules [37,38]. Recently, the concept of protein expression pattern/signature (PES) evolved from these human clinical proteomics has been increasingly applied in environmentally relevant organisms [15–17,32]. PES is defined as a set of proteins as biomarkers of specific environmental stressors. The characteristic PES in the unsequenced animals is independent of the identity of the proteins and may be a robust discriminator of a specific pollutant in real contaminated environments. In the present study, we obtained a PES composing of 13 commonly altered protein spots in the two metal-contaminated oyster populations, and multivariate clustering analyses were employed to blindly classify oysters with similar proteome expression patterns into the same class (Fig. 3C). Clearly, the results showed that the clean ZP oysters formed a separate cluster while the GQ and BJ contaminated ones were clustered

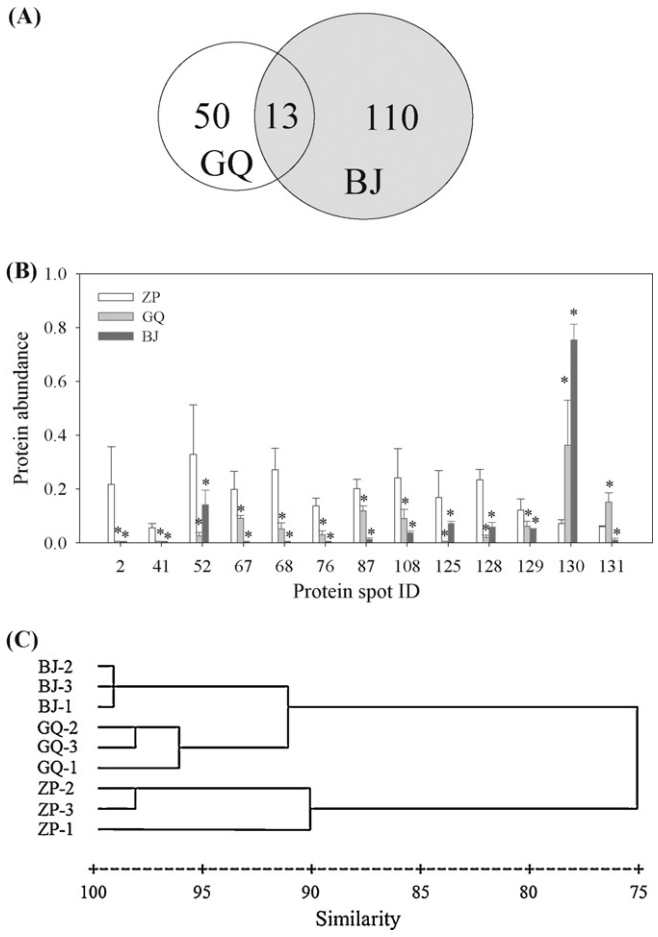

Fig. 3. (A) Venn diagram showing the number of the differentially expressed gill proteins for the metal-contaminated oysters (i.e., GQ and BJ) in comparison with the clean ones (ZP) ($P < 0.05$, Student t-test). (B) Expression abundance of the 13 differentially expressed protein spots in the gill of the oysters from the metal-contaminated (GQ and BJ) and clean (ZP) sites. Mean ± standard deviation ($n = 3$). Protein spot ID refers to the labeled number in the Fig. 2. *indicates significant difference with that in the ZP ($P < 0.05$, Student t-test). (C) Hierarchical clustering of the 13 commonly altered proteins and each representing one biological replicate. The dendrogram provides a measure of the relatedness of protein expression pattern.

together, and the highly contaminated BJ ones had lower similarity levels to the ZP ones than the less contaminated GQ ones (Fig. 3C). Amelina et al. [17] also reported that the clean mussels *Mytilus edulis* could be distinguished from the contaminated ones based on a PES composed of 13 proteins. Apraiz et al. [16] described PES in *M. edulis* exposed to individual marine pollutants, and these single pollutant-specific PESs had particular diagnostic value in environmental pollution monitoring programs.

The second question was that whether proteome pattern can diagnose health status of these biomonitors. Here, we aimed to test whether there was a meaningful relationship between the pattern changes of gill proteome and the integrated contamination of the metals/metalloid (possibly integrated toxic effect) in the field-collected oysters. In order to do this, we began with a simple assumption that the integrated toxic effect of the metals/metalloid is the sum of the resultant toxicity from each one (i.e., tissue residue addition approach). But, much work is needed to test whether there are different patterns of intracellular interactions between the metals on the integrated metal toxicity. The integrated proteome change can be calculated from the follow equation:

$$\text{Integrated proteome change} = \sum_{j=1}^{n} |C^{j}_{\text{contaminated}} - C^{j}_{\text{clean}}|$$

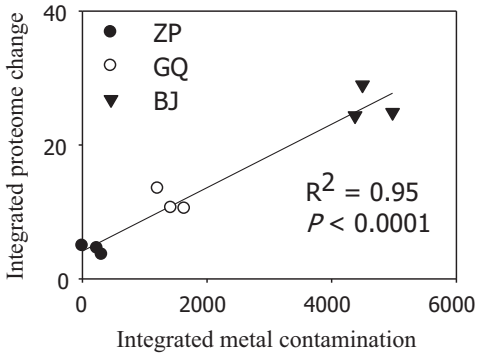

Fig. 4. Relationship between the 'Integrated proteome change' and the 'Integrated metal contamination' or 'Integrated metal toxic effect' (*see text for the calculation*) in the gill of the oysters, and each dot represents one biological replicate.

where $C^{j}_{\text{contaminated}}$ is the normalized concentration of the jth differentially expressed protein spot in a contaminated oyster, C^{j}_{clean} is the normalized concentration of the jth protein in an uncontaminated one, and n is the number of the differentially expressed protein. In the present study, the values of j were 63 and 123 for the GQ and the BJ, respectively. We found that the intra-population variations in the integrated proteome change were small (Fig. 4), and the relative standard deviations were 15.5% for the ZP, 14.8% for the GQ, and 9.7% for the BJ. Importantly, the inter-population variations significantly differed from each other, and the order of the integrated proteome change, i.e., the BJ oysters > the GQ oysters > the ZP oysters, was in good agreement with the order of the integrated metal contamination (possibly the integrated toxic effect).

Clearly, there was a linear relationship between the integrated proteome change and the integrated metal contamination observed in the oysters ($R^2 = 0.95$, $P < 0.0001$, Fig. 4). The relationship suggested that proteome change in abundance may have a strong predictive power of pollution and toxic effects of metals/metalloids. Here, the central hypothesis was that the relative expression abundance of proteome in a target organ reflected the ongoing events involved in toxicant responses, and thus the pattern change of the proteome could comprehensively characterize the extent of toxic effects on the organism. The predictive power of the toxic effect of metals/metalloids by using proteome pattern may be further improved if the cellular metal-metal interactions, missing proteins/peptides, protein post-translational modifications and re-localization are considered.

3.3. Protein identification in the oysters

Environmental proteomics is increasingly employed to elucidate the underlying molecular mechanisms of toxicant responses by aquatic organisms [6–8,14,39]. For a better understanding of the mode of action of aquatic pollutants, successful identification of metal-altered proteins is a prerequisite in these animals with unsequenced genomes. The mass spectrometry (MS) technology followed by homology searches has been successfully developed for protein identification in many organisms with non-sequenced genomes [40], and novel proteins participating in diverse biological processes have been identified and proposed as novel biomarkers of metal exposure [16,21,32,41]. In the present study, all the differentially expressed proteins, i.e., 173 spots, were submitted for putative identification by a MALDI-TOF/TOF MS/MS analysis and followed by homology searches in the NCBInr and bivalvia EST databases, since the genetic sequences of the oyster are absent from the databases at present. In the preliminary effort at protein identification, the majority of the spots were not identified,

Table 2
Putative identification of the differentially expressed proteins in the gill of the oysters *Crassostrea hongkongensis* collected from the metal-contaminated GQ and BJ sites, in comparison to those in the clean ZP oysters.

Spot ID[a]	Fold change[b]		Protein identity	Species[c]	Accession number[d]	Theoretical MW (kDa)/pI[e]	Peptides count	Biological process
	GQ	BJ						
ZP-17	−14.7	–	Methionine adenosyltransferase	*Childia* sp. MR-2009	gi|255733356	35256.7/5.38	4	Amino acid metabolism
ZP-58	–	ND	Beta-actin	*Liposcelis paeta*	gi|258617817	31334.6/5.14	3	Cell structure and motility
ZP-60	–	ND	Actin	*Ciona intestinalis*	gi|198424630	41913.9/5.29	6	Cell structure and motility
ZP-75	–	ND	Mitochondrial H^+ ATPase a subunit	*Pinctada fucata*	gi|116008297	59813.6/8.92	18	ATP synthesis
ZP-77	–	ND	Predicted: hypothetical protein	*Monodelphis domestica*	gi|126326243	37272.7/6.41	2	Unknown
ZP-82	–	ND	Prohibitin, putative	*Ixodes scapularis*	gi|241065293	29117.2/6.02	4	Mitochondrial function, transcription, etc.
ZP-102	–	-2.6	Phosphorylase phosphatase	*Xenopus laevis*	gi|963085	66066.2/4.83	8	Signal transduction, transcription, metabolism, etc.
ZP-106	–	−2.6	26S protease regulatory subunit 6A, putative	*Pediculus humanus corporis*	gi|242004678	42523.1/5.63	9	Proteolysis
ZP-112	–	5.5	Enolase	*Phytophthora infestans* T30-4	gi|301118044	49416.2/5.25	5	Glycolysis
ZP-114	–	−4.6	CRE-PGK-1 protein	*Caenorhabditis remanei*	gi|308505762	44217.2/6.34	7	Unknown
ZP-115	–	−3.4	Medium-chain acyl-CoA dehydrogenase	*Chiloscyllium plagiosum*	gi|298155806	25314/8.89	6	Fatty acid metabolism
ZP-116	–	−1.9	4-hydroxyphenylpyruvate dioxygenase	*Paracoccidioides brasiliensis* Pb18	gi|226288135	45874.1/5.64	4	Amino acid metabolism
ZP-120	−7.3	–	Elongation factor 2	*Suberites fuscus*	gi|32967436	28600.5/6.03	6	Protein biosynthesis
GQ-2	New	–	Extracellular superoxide dismutase	*Saccostrea glomerata*	gi|229485195	21666.1/5.27	3	Superoxide metabolism
GQ-13	New	–	Manganese-superoxide dismutase	*Scapharca broughtonii*	gi|253684161	21186.8/6.11	3	Superoxide metabolism
BJ-1	–	New	Calreticulin	*Crassostrea gigas*	gi|148717307	48499.3/4.53	13	Protein degradation, transcription regulation, etc.
BJ-5	–	New	Malate dehydrogenase precursor	*Nucella lapillus*	gi|6746611	36590.4/8.44	5	Tricarboxylic acid cycle
BJ-7	–	New	Hemocyte extracellular superoxide dismutase	*Crassostrea gigas*	gi|66970169	21423.8/4.84	1	Superoxide metabolism
BJ-9	–	New	Hemocyte extracellular superoxide dismutase	*Crassostrea gigas*	AAY60161.1	26706.3/5.03	1	Superoxide metabolism

[a] Spot ID refers to the labeled number in the gels of Fig. 2.
[b] Fold change was calculated by dividing expression abundance in the contaminated oysters by that observed in the clean ZP, and the down-regulated proteins were assigned negative reciprocals. Values are only shown for significant differences ($P < 0.05$, Student's *t*-test). '–' indicates no significant difference with that of the ZP. 'ND' indicates non-detectable, and 'New' indicates newly appearing.
[c] Species in which proteins were identified.
[d] Accession number from National Center for Biotechnology Information database.
[e] MW = molecular weight; p*I* = isoelectric point.

mainly due to the lack of genomic information, the too low spot abundance, or the use of the MALDI-TOF/TOF, although we were able to putatively identify 19 proteins (Table 2). Thus, the use of more up to date instrumentation/bioinformatics such as nanoflow liquid chromatography-tandem mass spectrometry might improve the success rate of protein identification in the oysters [20,23]. The fold change, theoretical molecular weight and p*I*, peptide species count and biological function of the 19 proteins are reported in Table 2.

The identified proteins are involved in a variety of biological processes, such as amino acid metabolism, ATP synthesis, cell structure and motility, glycolysis, fatty acid metabolism, protein biosynthesis, protein degradation, tricarboxylic acid cycle, and superoxide metabolism (Table 2). It appears that the systemic cellular dysfunctions were associated with multiple-metal exposure, and the disorders might be partly associated with the reduced growth rates observed in the contaminated populations [25]. Firstly, we found that the expression of medium-chain acyl-CoA dehydrogenases decreased by 3.4-fold in the BJ oysters. It is known that the deficiencies in acyl-CoA dehydrogenases can result in an insufficiency in fatty acids oxidization, thus consequently leading to an inability to gain energy and make sugar from fat stores [42]. Secondly,

metabolic disorder of amino acids may occur in the oysters under metal stress, since there was down-regulation of two important enzymes, i.e., 4-hydroxyphenylpyruvate dioxygenase (HPPD) and methionine adenosyltransferase (MA). The HPPD, a Fe-containing enzyme, functions in the catabolism of tyrosine [43], was decreased by 1.9-fold in the BJ oysters. The MA, with an important function in producing S-adenosylmethionine (SAM) [44], was down-regulated by 14.7-fold in the GQ oysters. The inhibition of SAM cycle may partly contribute to the observed slow growth rate of the metal-exposed oysters, since SAM is required for cellular growth [45]. Thirdly, we observed differential expression of actin proteins in the BJ animals but not in the GQ ones. Actins are highly conserved proteins participating in many important biological processes such as muscle contraction, cell motility, cell integrity [46]. The altered expression of the proteins probably disrupted normal physiological functions of the gill in food gathering, respiration and nutrient requisition. However, the frequently reported cytoskeletal proteins may not be specific to metal stress, and they probably represent common cellular stress responses [47]. Finally, the highly contaminated BJ oysters had a significantly lower expression of mitochondrial H^+ ATPase, which is crucial in ATP metabolism. The suppressed ATP production could probably affect nutrient uptake and maintenance of transmembrane proton gradient for transport of the nutrients into the cells [48].

Likely, the oysters had employed specific cellular strategies for metal detoxification, making them tolerant of such high concentrations of bioaccumulated metals, especially Cu, Zn and Cd. Firstly, the GQ and BJ populations showed remarkable expression of superoxide dismutase (SOD), which is the first line of defense against reactive oxygen species resulted from metal over-load [49]. The second approach was probably by improving energy production for metal sequestration/detoxification, as indicated by the significant increases of enolase and malate dehydrogenase precursor in the BJ oysters [50,51]. Thirdly, subcellular fractionation analysis revealed that only a negligible fraction of Cu and Zn was distributed into cellular metal-sensitive fractions [24]. Indeed, a previous ultrastructural study of metal-contaminated oysters found that Cu and Zn were immobilized in membrane-limited vesicles as different chemical compounds [52].

4. Conclusion

In conclusion, the present study revealed that proteome pattern is a powerful discriminator of metal contamination in biomonitors, and it is also useful in contamination classification. A further robust identification/verification of the altered proteins may lead to the discovery of novel specific biomarkers, which shall significantly improve our ability in metal pollution assessment. We also found that the integrated pattern change of gill proteome correlated linearly with the integrated contamination or toxic effect of the metals/metalloid, suggesting that proteome pattern may be a good indicator of contamination or toxicity of metal mixtures in the aquatic organisms.

Acknowledgements

We thank the anonymous reviewers for their helpful comments on this work. This study was supported by a Key Project from the Natural Science Foundation of China (no. 21237004).

References

[1] S.N. Luoma, P.S. Rainbow, Metal Contamination in Aquatic Environments: Science and Lateral Management, Cambridge University Press, New York, 2008.
[2] P.S. Rainbow, Biomonitoring of heavy metal availability in the marine environment, Mar. Pollut. Bull. 31 (1995) 183–192.
[3] E.D. Goldberg, V.T. Bowen, J.W. Farrington, G. Harvey, J.H. Martin, P.L. Parker, R.W. Risebrough, W. Robertson, E. Schneider, E. Gamble, The mussel watch, Environ. Conserv. 5 (1978) 101–125.
[4] M.H. Depledge, M.C. Fossi, The role of biomarkers in environmental assessment. II. Invertebrates, Ecotoxicology 3 (1994) 161–172.
[5] T.S. Galloway, R.J. Brown, M.A. Browne, A. Dissanayake, D. Lowe, M.B. Jones, M.H. Depledge, A multibiomarker approach to environmental assessment, Environ. Sci. Technol. 38 (2004) 1723–1731.
[6] B.A. Wetmore, B.A. Merrick, Toxicoproteomics: proteomics applied to toxicology and pathology, Toxicol. Pathol. 32 (2004) 619–642.
[7] T. Monsinjon, T. Knigge, Proteomic applications in ecotoxicology, Proteomics 7 (2007) 2997–3009.
[8] M.F.L. Lemos, A.M.V.M. Soares, A.C. Correia, A.C. Esteves, Proteins in ecotoxicology – how, why and why not? Proteomics 10 (2010) 873–887.
[9] V.E. Forbes, A. Palmqvist, L. Bach, The use and misuse of biomarkers in ecotoxicology, Environ. Toxicol. Chem. 25 (2006) 272–280.
[10] J.C. Amiard, C. Amiard-Triquet, S. Barka, J. Pellerin, P.S. Rainbow, Metallothioneins in aquatic invertebrates: their role in metal detoxification and their use as biomarkers, Aquat. Toxicol. 76 (2006) 160–202.
[11] F. Liu, W.-X. Wang, Metallothionein-like proteins turnover, cadmium and zinc biokinetics in the dietary Cd-exposed scallop *Chlamys nobilis*, Aquat. Toxicol. 105 (2011) 361–368.
[12] R.I.L. Eggen, R. Behra, P. Burkhardt-Holm, B.I. Escher, N. Schweigert, Challenges in ecotoxicology, Environ. Sci. Technol. 38 (2004) 58A–64A.
[13] J.R. Snape, S.J. Maund, D.B. Pickford, T.H. Hutchinson, Ecotoxicogenomics: the challenge of integrating genomics into aquatic and terrestrial ecotoxicology, Aquat. Toxicol. 67 (2004) 143–154.
[14] V.J. Nesatyy, M.J.F. Suter, Proteomics for the analysis of environmental stress responses in organisms, Environ. Sci. Technol. 41 (2007) 6891–6900.
[15] J.L. Shepard, B. Olsson, M. Tedengren, B.P. Bradley, Protein expression signatures identified in *Mytilus edulis* exposed to PCBs, copper and salinity stress, Mar. Environ. Res. 50 (2000) 337–340.
[16] I. Apraiz, J. Mi, S. Cristobal, Identification of proteomic signatures of exposure to marine pollutants in mussels (*Mytilus edulis*), Mol. Cell. Proteomics 5 (2006) 1274–1285.
[17] H. Amelina, I. Apraiz, W. Sun, S. Cristobal, Proteomics-based method for the assessment of marine pollution using liquid chromatography coupled with two-dimensional electrophoresis, J. Proteome Res. 6 (2007) 2094–2104.
[18] L. Tomanek, M.J. Zuzow, A.V. Ivanina, E. Beniash, I.M. Sokolova, Proteomic response to elevated P_{CO_2} level in eastern oysters Crassostrea virginica: evidence for oxidative stress, J. Exp. Biol. 214 (2011) 1836–1844.
[19] E.L. Thompson, D.A. Taylor, S.V. Nair, G. Birch, P.A. Haynes, D.A. Raftos, Proteomic discovery of biomarkers of metal contamination in Sydney rock oysters (*Saccostrea glomerata*), Aquat. Toxicol. 109 (2012) 202–212.
[20] S. Muralidharan, E.L. Thompson, D. Raftos, G. Birch, P.A. Haynes, Quantitative proteomics of heavy metal stress responses in Sydney rock oysters, Proteomics 12 (2012) 906–921.
[21] A. Romero-Ruiz, M. Carrascal, J. Alhama, J.L. Gómez-Ariza, J. Abian, J. López-Barea, Utility of proteomics to assess pollutant response of clams from the Doñana bank of Guadalquivir Estuary (SW Spain), Proteomics 6 (2006) S245–S255.
[22] B.C. Sanchez, K. Ralston-Hooper, M.S. Sepúlveda, Review of recent proteomic applications in aquatic toxicology, Environ. Toxicol. Chem. 30 (2011) 274–282.
[23] E.L. Thompson, D.A. Taylor, S.V. Nair, G. Birch, G.C. Hose, D.A. Raftos, Proteomic analysis of Sydney rock oysters (*Saccostrea glomerata*) exposed to metal contamination in the field, Environ. Pollut. 170 (2012) 102–112.
[24] W.-X. Wang, Y. Yang, X. Guo, M. He, F. Guo, C. Ke, Copper and zinc contamination in oysters: subcellular distribution and detoxification, Environ. Toxicol. Chem. 30 (2011) 1767–1774.
[25] K. Pan, W.-X. Wang, Reconstructing the biokinetic processes of oysters to counteract the metal challenges: resistance development, Environ. Sci. Technol. (2012), http://dx.doi.org/10.1021/es302040g.
[26] G. Li, Z. Cao, D. Lan, J. Xu, S. Wang, W. Yin, Spatial variations in grain size distribution and selected metal contents in the Xiamen Bay, China, Environ. Geol. 52 (2007) 1559–1567.
[27] L. Zhang, X. Ye, H. Feng, Y. Jing, T. Ouyang, X. Yu, R. Liang, C. Gao, W. Chen, Heavy metal contamination in western Xiamen Bay sediments and its vicinity, China, Mar. Pollut. Bull. 54 (2007) 974–982.
[28] W. Chen, L. Zhang, L. Xu, X. Wang, L. Hong, H. Hong, Residue levels of HCHs, DDTs and PCBs in shellfish from coastal areas of east Xiamen Island and Minjiang estuary, China, Mar. Pollut. Bull. 45 (2002) 385–390.
[29] D.W. Klumpp, H. Hong, C. Humphrey, X. Wang, S. Codi, Toxic contaminants and their biological effects in coastal waters of Xiamen, China. I. Organic pollutants in mussel and fish tissues, Mar. Pollut. Bull. 44 (2002) 752–760.
[30] X. Wang, H. Hong, L. Xu, W. Chen, Z. Zhang, Distribution and transportation of polycyclic aromatic hydrocarbons in suspended particulate matter and surface sediment from the Pearl River estuary, J. Environ. Sci. Health A 37 (2002) 451–463.
[31] X. Wang, L. Xu, W. Chen, L. Zhang, H. Hong, The vertical distribution of PAHs and the tracing of pollutants in sediments of Xiamen bay, China Environ. Sci. 17 (1997) 19–22.
[32] F. Liu, D.Z. Wang, W.-X. Wang, Cadmium-induced changes in trace element bioaccumulation and proteomics perspective in four marine bivalves, Environ. Toxicol. Chem. 31 (2012) 1292–1300.

[33] A.P. Diz, E. Dudley, B.W. MacDonald, B. Piña, E.L.R. Kenchington, E. Zouros, D.O.F. Skibinski, Genetic variation underlying protein expression in eggs of the marine mussel *Mytilus edulis*, Mol. Cell. Proteomics 8 (2009) 132–144.
[34] J.P. Shine, R.V. Ika, T.E. Ford, Multivariate statistical examination of spatial and temporal patterns of heavy metal contamination in New Bedford Harbor marine sediments, Environ. Sci. Technol. 29 (1995) 1781–1788.
[35] A. Field, Discovering Statistics Using SPSS, second ed., SAGE Publications, London, 2005.
[36] G.M. Kruzynski, Cadmium in oysters and scallops: the BC experience, Toxicol. Lett. 148 (2004) 159–169.
[37] T.R. Golub, D.K. Slonim, P. Tamayo, C. Huard, M. Gaasenbeek, J.P. Mesirov, H. Coller, M.L. Loh, J.R. Downing, M.A. Caligiuri, C.D. Bloomfield, E.S. Lander, Molecular classification of cancer: class discovery and class prediction by gene expression monitoring, Science 286 (1999) 531–537.
[38] E.F. Petricoin III, A.M. Ardekani, B.A. Hitt, P.J. Levine, V.A. Fusaro, S.M. Steinberg, G.B. Mills, C. Simone, D.A. Fishman, E.C. Kohn, L.A. Liotta, Use of proteomic patterns in serum to identify ovarian cancer, Lancet 359 (2002) 572–577.
[39] F. Marsano, L. Boatti, E. Ranzato, M. Cavaletto, V. Magnelli, F. Dondero, A. Viarengo, Effects of mercury on *Dictyostelium discoideum*: proteomics reveals the molecular mechanisms of physiological adaptation and toxicity, J. Proteome Res. 9 (2010) 2839–2854.
[40] A. Shevchenko, S. Sunyaev, A. Loboda, A. Shevchenko, P. Bork, W. Ens, K.G. Standing, Charting the proteomes of organisms with unsequenced genomes by MALDI-quadrupole time-of-flight mass spectrometry and BLAST homology searching, Anal. Chem. 73 (2001) 1917–1926.
[41] S. Chora, M. Starita-Geribaldi, J.M. Guigonis, M. Samson, M. Roméo, M.J. Bebianno, Effect of cadmium in the clam *Ruditapes decussatus* assessed by proteomic analysis, Aquat. Toxicol. 94 (2009) 300–308.
[42] C. Thorpe, J.J. Kim, Structure and mechanism of action of the acyl-CoA dehydrogenases, FASEB J. 9 (1995) 718–725.
[43] K. Johnson-Winters, V.M. Purpero, M. Kavana, T. Nelson, G.R. Moran, (4-Hydroxyphenyl) pyruvate dioxygenase from *Streptomyces avermitilis*: the basis for ordered substrate addition, Biochemistry 42 (2003) 2072–2080.
[44] G.L. Cantoni, The nature of the active methyl donor formed enzymatically from L-methionine and adenosinetriphosphate, J. Am. Chem. Soc. 74 (1952) 2942–2943.
[45] W.A.M. Loenen, S-adenosylmethionine: jack of all trades and master of everything? Biochem. Soc. Trans. 34 (2006) 330–333.
[46] T.D. Pollard, J.A. Cooper, Actin and actin-binding proteins – a critical-evaluation of mechanisms and functions, Annu. Rev. Biochem. 55 (1986) 987–1035.
[47] J. Petrak, R. Ivanek, O. Toman, R. Cmejla, J. Cmejlova, D. Vyoral, J. Zivny, C.D. Vulpe, Déjà vu in proteomics. A hit parade of repeatedly identified differentially expressed proteins, Proteomics 8 (2008) 1744–1749.
[48] P.D. Boyer, The ATP synthase – a splendid molecular machine, Annu. Rev. Biochem. 66 (1997) 717–749.
[49] F. Regoli, Chemical pollutants and the mechanisms of reactive oxygen species generation in aquatic organisms, in: D. Abele, J.P. Vázquez-Medina, Zenteno-Savín (Eds.), Oxidative Stress in Aquatic Ecosystems, John Wiley & Sons, Ltd., Chichester, 2011, http://dx.doi.org/10.1002/9781444345988.ch22.
[50] P.C. Babbitt, M.S. Hasson, J.E. Wedekind, D.R. Palmer, W.C. Barrett, G.H. Reed, I. Rayment, D. Ringe, G.L. Kenyon, J.A. Gerlt, The enolase superfamily: a general strategy for enzyme-catalyzed abstraction of the alpha-protons of carboxylic acids, Biochemistry 35 (1996) 16489–16501.
[51] P. Minárik, N. Tomáková, M. Kollárová, M. Antalík, Malate dehydrogenases-structure and function, Gen. Physiol. Biophys. 21 (2002) 257–265.
[52] J.D. Thomson, B.J.S. Pirie, S.G. George, Cellular metal distribution in the Pacific oyster *Crassostrea gigas* (Thun.) determined by quantitative X-ray microprobe analysis, J. Exp. Mar. Biol. Ecol. 85 (1985) 37–45.